

OPEN

Inhibition of snake venom induced sterile inflammation and PLA2 activity by Titanium dioxide Nanoparticles in experimental animals

Shubhro Chakrabarty¹, Md. Iqbal Alam², Saumya Bhagat³, Aftab Alam⁴, Neha Dhyani², Gausal A. Khan³ & M. Sarwar Alam⁵

Sterile inflammation (SI) is an essential process in response to snakebite and injury. The venom induced pathophysiological response to sterile inflammation results into many harmful and deleterious effects that ultimately leads to death. The available treatment for snakebite is antiserum which does not provide enough protection against venom-induced pathophysiological changes like haemorrhage, necrosis, nephrotoxicity and often develop hypersensitive reactions. In order to overcome these hindrances, scientists around the globe are searching for an alternative therapy to provide better treatment to the snake envenomation patients. In the present study TiO₂ (Titanium dioxide)-NPs (Nanoparticles) has been assessed for antisnake venom activity and its potential to be used as an antidote. In this study, the synthesis of TiO₂-NPs arrays has been demonstrated on p-type Silicon Si < 100 > substrate (~30 ohm-cm) and the surface topography has been detected by Field-emission scanning electron microscopy (FESEM). The TiO₂-NPs successfully neutralized the *Daboia russelii* venom (DRV) and *Naja kaouthia* venom (NKV)-induced lethal activity. Viper venom induced haemorrhagic, coagulant and anticoagulant activities were effectively neutralized both in *in-vitro* and *in vivo* studies. The cobra and viper venoms-induced sterile inflammatory molecules (IL-6, HMGB1, HSP70, HSP90, S100B and vWF) were effectively neutralised by the TiO₂-NPs in experimental animals.

Biomedical therapy and diagnostics are getting more prominent with the utilization of nanotechnology concept¹. The aim of using a nano-medicine is to improve the bio-distribution of therapeutic agent and to allow its accumulation on the target site². Different types of nano-medicine have been evaluated in recent years, f.e., liposomes, polymers, micelles and antibodies. Several evidences also indicate the ability of these nano-sized carrier materials to improve the balance between the efficacy and the toxicity of therapeutic interventions.

Today, nano-scale research has been emerged as important players in the field of pharmacology and biotechnology. Except few nanoparticles and quantum dots, most of them are toxic in nature and are not applicable for medical or therapeutic applications³. TiO₂ has a wide spectrum of properties that varies with different techniques used for its synthesis⁴ and has applications in the field of biomedical research and treatment such as anti-tumour therapy^{5,6}, manufacturing of bio-products⁷ etc. Ubiquitous applications and better results of TiO₂-NPs, makes them a potential candidate for biomedical research⁸. In the present study, the synthesis of TiO₂-NPs arrays has been demonstrated on p-type Silicon Si < 100 > substrate (~30 ohm-cm) and the surface topography has been detected by Field-emission scanning electron microscopy (FESEM). The size of the deposited TiO₂-NPs is maximum in the range of 5–6 nm. The Energy-Dispersive X-ray (EDX) mapping of FESEM image showed the presence

¹Department of Electronics and Communication Engineering, NIT, Goa, India. ²Department of Physiology, Hamdard Institute of Medical Sciences & Research, Jamia Hamdard, New Delhi, India. ³Hematology division, Defence Institute of Physiology and Allied Sciences, DRDO, Delhi, India. ⁴Division of Neurosurgery, Department of Clinical Neurosciences, University of Cambridge, Cambridge, UK. ⁵Department of Chemistry, School of Chemical and Life Sciences, Jamia Hamdard, New Delhi, India. Correspondence and requests for materials should be addressed to M.I.A. (email: iqbalasc@yahoo.com)

of Titanium (Ti), Oxygen (O₂) and Si (Substrate) in the sample. Raman analysis confirms the crystalline nature of TiO₂-NPs with Anatase and Rutile modes.

Present day lifestyle increases the risk of several deadly diseases including cardiovascular disorder, diabetes, cancer, etc. In these cases early detection and treatment can decrease the mortality rates. Apart from these lifestyle related diseases, some clinical conditions such as snake envenomation also pose a major public health challenge across the world. About 5.4 million annual snakebite cases are reported globally and more than 100,000 people die each year as a result of snakebites of which more than 50,000 deaths occur in India alone⁹. Majority of deaths reported are particularly from rural and agriculturally active areas. WHO has also declared snakebite as a 'neglected tropical disease' and is now a global health priority^{9–12}. Antiserum is the only choice to treat snakebite patients, which again is not always effective against venom-induced haemorrhage, necrosis, nephrotoxicity and often develop hypersensitive reaction^{13–17}. Antiserum development in animal is time consuming and needs cold chain management. Therefore, there is a need to develop suitable therapeutic agent for the treatment of snakebite. Now-a-days use of nanoparticles are quite popular and frequently used as a drug-delivery vehicles^{2,18}. TiO₂ is one such promising material because of its wide spectrum properties that varies with different techniques used for its synthesis³ and has been reported for various applications in the field of biomedical research^{4–6}.

Sterile inflammation is an essential process in response to snakebite and injury. The pathophysiological response to sterile inflammation results into many harmful and deleterious effects that ultimately lead to death. The harmful effects of snake envenomation are haemorrhage, necrosis, renal failure, cardiotoxicity, neurotoxicity, myotoxicity and hematotoxicity. These deleterious effects could be due to the increased formation of sterile molecules: HMGB1, HSPs, S100B and IL6. HMGB1 which has recently been drawn much attention because of its binding ability to cell signalling receptors like RAGE, TLR2, TLR4 and TLR9 receptors. These receptors have major role in the initiation of inflammatory response and they also participate in development and progression of haemorrhage, necrosis, and cell death. Similar pathophysiological changes were also observed in case of snake envenomation. Therefore, in this paper we have shown the expression of the sterile inflammatory marker molecules developed in response to snakebite in experimental animals and its neutralization by TiO₂.

Materials

Chemicals. All chemical used in this study were of analytical grade. The solvents used were prepared in distilled water. Anti-Hsp70 antibody, Anti-Hsp90 antibody, Anti-IL-6 antibody, Anti-Von Willebrand Factor antibody, Anti-S100 beta antibody, Anti-HMGB1 antibody-ChIP Grade were purchased from Abcam (Cambridge, MA, USA); and O-Phenylenediamine dihydrochloride and bovine serum albumin were purchased from Sigma Aldrich (St. Louis, MO, USA). MaxiSorp flat-bottom 96-well plates were purchased from Nunc GmbH & Co, Langensfeld, Germany.

Methods

Animals. Male Swiss albino mice (18–20 g) used in this study was obtained from the animal house of Jamia Hamdard (Hamdard University), New Delhi. Guidelines of the Institutional Animal Ethical Committee has been followed for the care and handling of animals. All mice were housed five/cages and fed standard laboratory diet and water *ad libitum* with 12-h dark/light cycles at constant temperature of 25 ± 2 °C. 'Principles of laboratory animal care' (NIH publication No. 85-23, revised in 1985) as well as Indian laws on 'Protection of Animals' have been followed for all the animal experiments under the provision of authorized investigators. Experiments involving the use of mice were approved by the Committee for the Purpose of Control and Supervision of Experiments on Animals (CPCSEA) of the Jamia Hamdard (Deemed University), New Delhi (permission #173/GO/Re/S/2000/CPCSEA). Experiments involving animals meet the International Guiding Principles for Biomedical Research Involving Animals (CIOMS).

Preparation of nanoparticles. The GLAD technique was carried out to deposit TiO₂ (High purity) (99.99%, MTI, USA) NPs of 5 nm range inside the electron beam chamber (Hind High Vacuum Co. (p) Ltd., 15F6) on p-type Silicon Si <100> substrate (~30 ohm-cm) at a base pressure of ~2 × 10⁻⁵ mbar¹⁹. The substrates were rotated azimuthally with constant speed of 460 rpm at an orientation of 85° with respect to the perpendicular line between the metal source and the planar substrate holder²⁰. A low deposition rate of 1.2 Å/s was kept constant, which was monitored by a quartz crystal. Then the grown TiO₂-NPs were ultrasonicated in electron grade acetone to make a liquid solution. The surface morphology of randomly placed TiO₂-NPs over n-type Si substrate of probably 5 nm was observed using an Atomic Force Microscope (BrukerInnova).

Preparation of venoms. Lyophilized snake venom from *Daboia russelii* (Viper), and *Naja kaouthia* (Cobra) were obtained from Calcutta Snake Park (Kolkata, India) and was preserved in desiccators at 4 °C in an amber-coloured glass vial until further use. The snake venom was dissolved in 0.9% saline and centrifuged at 2000 rpm for 10 min. The supernatant was used as venom and kept at 4 °C and used within three month. The venom concentration was expressed in terms of dry weight (mg/ml, stock venom solution)²¹.

Venom inhibiting activity. To determine the venom inhibiting activity of the nanoparticles, following pharmacological experiments were performed:

Inhibition of venom lethal effect. Snake venom toxicity assessment was done by intravenous (*i.v*) injection of venom prepared in 0.2 mL physiological saline at different concentration in male albino mice weighing 18–20 g^{22,23}. Assessment of *in vitro* antagonism was done by mixing different concentrations of venom (2.2–22 µg) with a fixed amount of TiO₂-NPs, the mixture incubated at 37 °C for 1 hour, and then centrifuged at 2000 rpm for 10 minutes. The supernatant was injected intravenously (*i.v*) into male albino mice, six mice per dose. The median lethal dose (MLD₅₀) was calculated 24 hours after injection of the venom-TiO₂-NPs mixture. Lethal toxicity was also assessed

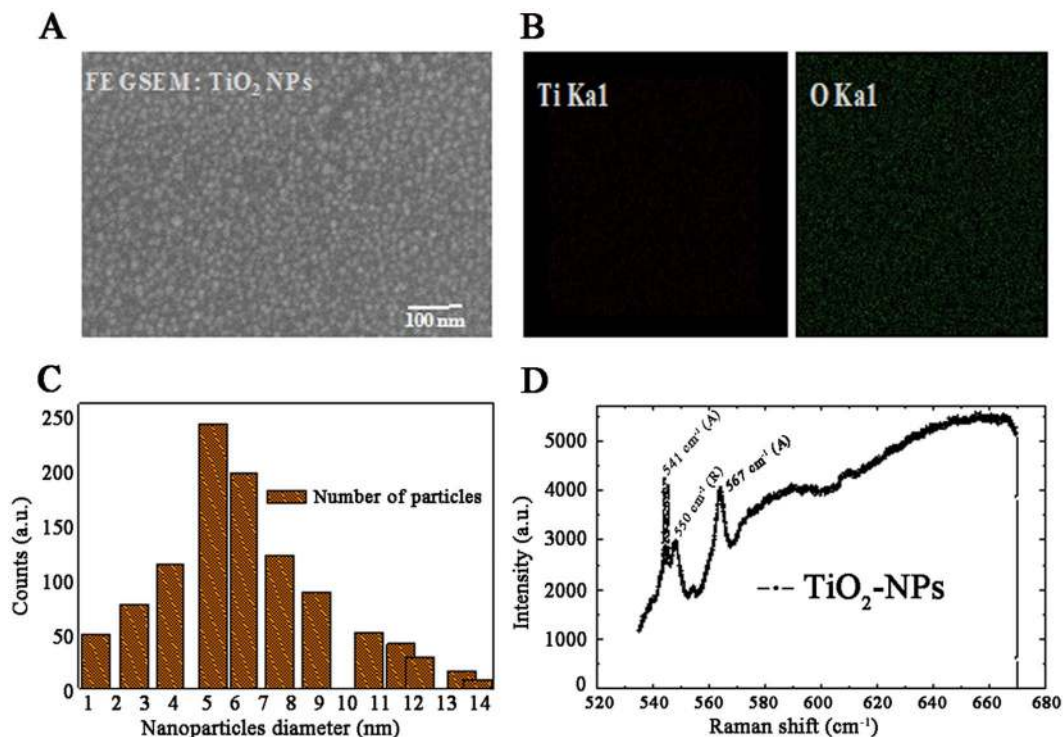


Figure 1. Structural behaviour of TiO₂-NPs. (A) Top view FESEM images of nano-sized TiO₂ particles. (B) Element mapping of the sample. (C) Particle histogram of Image 1(A). (D) Raman spectrum of TiO₂-NPs.

by subcutaneous (*s.c*) injection of various doses of venom. The neutralizing potency of TiO₂-NPs was assessed by injection (*s.c*) of venom (45–225 µg) into groups of six mice followed by immediate injection of fixed dose of TiO₂-NPs (5 ng) intravenously²⁴.

Inhibition of venom haemorrhagic activity. The minimum haemorrhagic dose (MHD) of venom which when administered into mice causes development of haemorrhagic lesion of 10 mm diameter within 24 hours²³. This lesion was measured and the estimation of neutralization of the haemorrhagic activity was done by mixing a fixed amount of TiO₂-NPs (2 ng) with different amounts of venom (5–25 µg). The mixture of TiO₂-NPs- venom was incubated at 37 °C for 1 hour, then spin at 2000 rpm for 10 min and finally 0.1 ml of supernatant taken were injected intradermally (*i.d*)²⁵. After 24 hours haemorrhagic lesion was estimated. To assess the anti-haemorrhagic activity of venom *in vivo*, various amount of venom (5–15 µg) were injected (*i.d*) followed by the TiO₂-NPs (5 ng, intravenously) and the haemorrhagic lesion measured after 24 hours.

Inhibition of venom necrotic activity. To assess the *in vitro* anti-necrosis effect of TiO₂-NPs, various concentration of venom (5–25 µg) were incubated with fixed amount of TiO₂-NPs and administered intradermally (*i.d*) into mice. The necrotic lesion was estimated after 48 hours. In *in vivo* study, the venom (*i.d*) (5–15 µg) was injected followed by injection (*i.v*) of TiO₂-NPs and observed after 48 hours.

Inhibition of venom defibrinogenating activity. Defibrinogenating activity of venoms or toxins is expressed as the minimum defibrinogenating dose (MDD). MDD of DRV is defined as the minimum amount of venom which when injected (intravenously) into mice causes incoagulable blood 1 hour later. Neutralization of this activity was estimated by mixing different amount of venom (2.5–12.5 µg) with fixed amounts of TiO₂-NPs, incubating at 37 °C for 1 hour and centrifugation. The supernatant was injected (*i.v*) into albino mice (18–20 g) as described above (*in vitro*). For *in vivo* studies, the MDD of venom was injected (*i.v*) followed by the TiO₂-NPs (*i.v*) and the nature of the blood observed after 1 hour²⁶.

Inhibition of venom PLA₂ effect. For carrying out the PLA₂ inhibition activity, 2 ml of egg yolk suspension, 0.2 ml of test material (venom, TiO₂-NPs and Venom + TiO₂-NPs) were mixed in the different test tube and kept for 1 hour incubation at 37 °C. The test tube containing test materials were kept on a water bath and the time required for coagulation was recorded. A blank was run with normal saline in place of test material. One unit enzyme activity was defined as the amount of venom, which increased the coagulation time of the egg yolk control by one minute²⁷. Estimation of neutralization of the enzyme activity, was done when fixed amount of TiO₂-NPs (2 ng) were mixed with different amount of viper venom (2–10 µg) and the mixture was incubated for 1 hour at 37 °C.

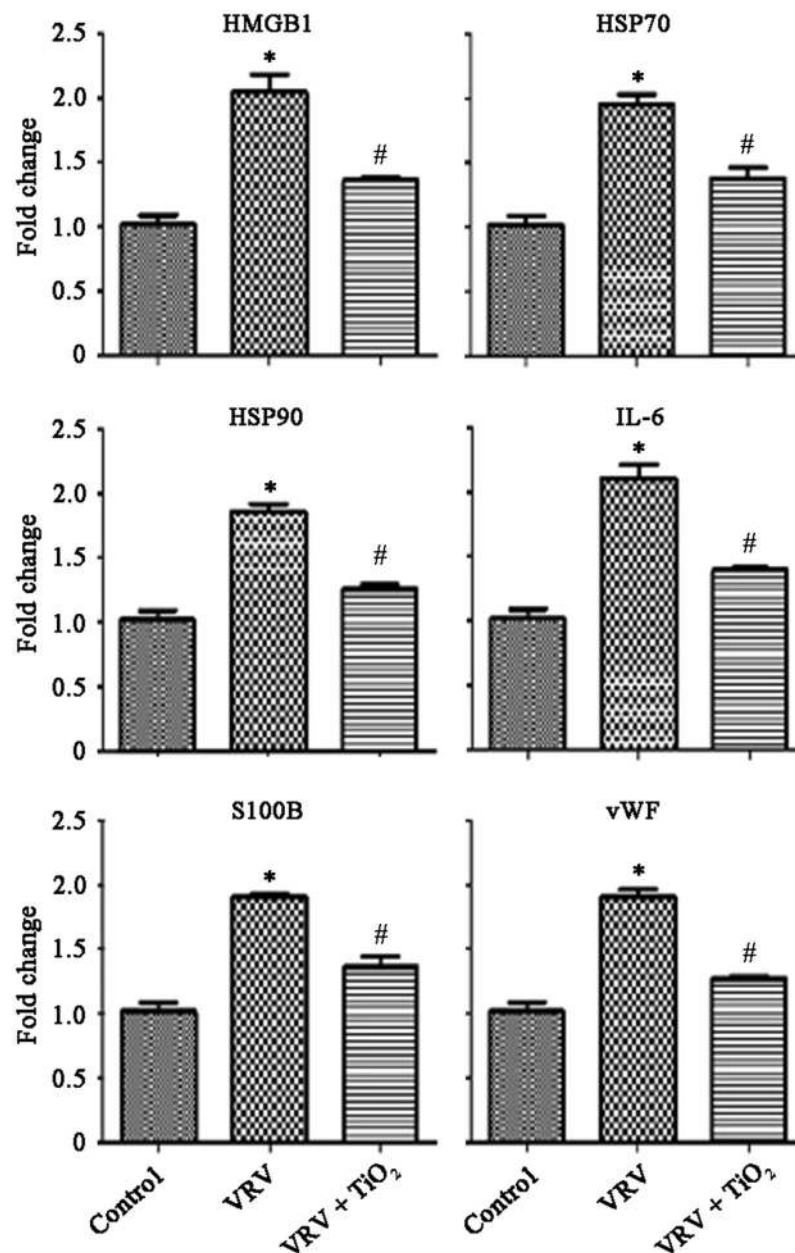


Figure 2. Viper (*Daboia russelii*) venom (VRV) induced inflammatory changes in experimental animals. Results expressed as mean \pm SEM (n = 6). Results obtained are significantly different from control group (*P < 0.05) and *Daboia russelii* venom (#P < 0.05).

Centrifuged at 2000 rpm for 10 minutes, supernatant was tested in a total of 0.2 ml for the enzyme neutralization activity.

Inhibition of venom-induced mouse paw oedema. The minimum oedematogenic dose (MOD) of venom/carrageenan is defined as the least amount of venom/carrageenan which when injected into male albino mice produced inflammation (oedema) in the paw. Non-fasted male albino mice (18–20 g) were treated with different doses of venom, carrageenan and TiO₂-NPs. To assess the anti-inflammatory activity of TiO₂-NPs various amount of venom/carrageenan (in 0.01 ml) were injected (intraplantar) followed by the intraperitoneal (*i.p.*) injection of TiO₂-NPs (250 ng/kg) and anti-inflammatory activity was measured. For control, equal amounts of saline were injected (intraplantar). The oedematogenic response was evaluated by the use of a screw gauge at given time intervals. Oedema was reported as the percentage difference between the values obtained from the injected paw with the carrageenan, venom, venom + TiO₂-NPs, carrageenan + TiO₂-NPs and saline, as described by Trebien and Calixto^{24,28}.

TiO ₂ (ng)	Viper Venom (μg)	Fold of neutralization (in terms of LD ₅₀)	Cobra Venom (μg)	Fold of neutralization (in terms of LD ₅₀)
Venom nano-particles incubated 37°C, 60 min and injected i.v				
TiO ₂ (2)	11	5	6	2.1
Control				
Venom injected (s.c) ** followed immediately by TiO₂ (i.v)				
TiO ₂ (5)	45	1.0	10	2.1

Table 1. Inhibition of lethal action of Viper and Cobra venom by TiO₂-NPs. Results are expressed as mean of six observations. **Duration of deaths time following venom exposure (venom control animal): DRV (1 Median Lethal Dose) = 13.24 ± 0.30 hours; Cobra (*Naja kaouthia*) venom (1 Median Lethal Dose) = 6.20 ± 0.30 hours.

TiO ₂ (ng)	Viper Venom μg)	Fold of neutralization (In terms of MHD)
Venom-TiO₂ nanoparticles incubated 37°C, 60 min and injected i.d		
TiO ₂ (2)	20	4
Venom injected (i.d) followed immediately by TiO₂ (i.v)		
TiO ₂ (5)	10	2

Table 2. Inhibition of haemorrhagic action of Viper venom by TiO₂-NPs. *Results are expressed as mean of six observations. *i.d* = intra-dermal. *i.v* = intra-venous.

TiO ₂ (ng)	Viper Venom (μg)	Fold of neutralization (In terms of MDD)
Venom-nanoparticles incubated 37°C, 60 min. and injected (i.v)		
TiO ₂ (2)	5.0	2.0
Venom injected (i.v) followed immediately by TiO₂		
TiO ₂ (5)	3.5	1.5

Table 3. Inhibition of defibrinogenating activity of Viper venom by TiO₂-NPs. *Results are expressed as mean of 6 observations. MDD = Minimum Defibrinogenating Dose = 2.5 μg.

Group	Viper Venom (μg)	Fold of neutralization (In terms of unit)
Control (only Venom)		
Viper (2 μg)	2(1)	1
Venom-NPs incubated 37°C, 60 min then added to egg yolk suspension		
TiO ₂ (2 ng)	10	5

Table 4. Inhibition of Phospholipase A₂ activity of Viper venom by TiO₂-NPs. Results are expressed as mean of ten observations. 1 unit = one unit of enzyme activity of DRV was defined as the amount of venom which increased the coagulation time of egg yolk by one minute.

Inhibition of Sterile inflammatory Markers. Different pro-inflammatory markers such as heat shock proteins (HSP70 and HSP90), high mobility group box 1 (HMGB1), interleukin 6 (IL-6), von Willbrand factor (vWF), and S100 calcium-binding protein B (S100B) was done by ELISA as described by Engvall *et al.*²⁹. Briefly, 50 μg of proteins were used with bicarbonate coating buffer to coat the wells in 96-well plates and incubated over night at 4 °C. Nonspecific binding was blocked with 5% BSA and then the samples were washed with PBST (0.05% Tween-20) and incubated for 3 hours with respective primary antibodies (against Hsp70; Hsp90; HMGB1); IL-6; vWF; S100b (1:1000). Next, the wells were washed and incubated with HRP conjugated secondary antibodies for 1 hour, and then washed with PBST and incubated with OPD substrate solution. The reaction was terminated by adding H₂SO₄ (1 N) and absorbance was measured at 450 nm. Using similar methods, a standard ELISA curve for absorbance versus specific antigen concentration was constructed using respective recombinant proteins.

Results

Topographic image of TiO₂-NPs. In case of GLAD, the TiO₂-NPs are formed due to the atomic shadowing effect on the arbitrarily deposited seeds. The diffusivity of the landed atoms on the substrate depends on the rate of evaporation. A lower evaporation rate of the material will enable the landed atoms to diffuse for longer distances before they get impinged by next arriving atoms. This can lead to an increase in the capture radius of the deposited atoms and hence the atoms nucleation area increases. Figure 1A shows a top view of grown TiO₂-NPs

Groups	Venom/Carrageenan µg (MED)	Oedema (%)			
		1 hour	2 hour	3 hour	4 hour
Control	(0.9% saline)				
Viper venom	001(1)	105.3 ± 5.8	87.5 ± 07.7	83.74 ± 5.9	78.43 ± 6.5
Carrageenan	300(1)	054.4 ± 7.2	47.9 ± 11.3	35.20 ± 7.6	34.60 ± 5.3
Inhibition studies (Carrageenan injected 300(1) into intraplantar surface followed immediately by TiO₂-NPs)					
TiO ₂ -NPs (250 ng/kg)	5(5)	47.5 ± 1.7	51.3 ± 2.5	52.0 ± 1.2	52.8 ± 2.9
Aspirin (10 mg/kg)	5(5)	43.9 ± 0.9	42.8 ± 1.2	42.2 ± 1.7	42.1 ± 0.8
Indomethacin (10 mg/kg)	5(5)	40.8 ± 1.9	40.3 ± 1.3	40.1 ± 0.5	39.9 ± 2.1
Inhibition studies (Carrageenan injected 300(1) intraplantar surface followed immediately by TiO₂-NPs)					
TiO ₂ -NPs (250 ng/kg)	600(2)	46.0 ± 1.8	49.6 ± 2.4	48.2 ± 1.6	48.0 ± 3.2
Aspirin (10 mg/kg)	600(2)	37.6 ± 2.7	42.6 ± 3.2	39.7 ± 2.7	40.1 ± 3.1
Indomethacin (10 mg/kg)	600(2)	35.1 ± 1.5	35.7 ± 2.8	35.3 ± 2.5	35.0 ± 1.4

Table 5. Viper venom induced inflammation and inhibition by TiO₂-NPs. Venom and carrageenan were injected intraplantar in the foot pads. Drugs were administered (*i.p*) immediately after envenomation at 0 hour.

on p-type Si substrate prepared at 85° and 460 rpm azimuthal rotation to the sample, the images were captured by FESEM, keeping the gun vacuum on 2.18 e-009 mBar. The EDX element mapping reveals Titanium (Ti, brown color) and Oxygen (O, green color) are present in the sample shown in Fig. 1B. Figure 1C projects the particle counts histogram of FEG: SEM image 1 A, the grown particles were in the range of 1–14 nm, where maximum number of NPs had a count of 5–6 nm. The Raman spectra processing of TiO₂ samples shows that the grown nanoparticles are having two Anatase and Rutile modes³⁰ (Fig. 1D).

Raman analysis. Raman spectroscopy is a flexible and most authenticated technique used for ubiquitous sectors. It is a very prominent tool for nano-biomedical studies and also helpful in the analysis of food and pharmaceutical non-materials. It has a great impact on drug analysis due to its simplicity in minimal sample handling and the significant differences in scattering strength between packaging materials tablet excipients, and active drug components³¹. Figure 1D shows the dependence of the Raman scattering intensity on the incident laser wavelength (laser excitation 532 nm). We have noticed that our prepared TiO₂-NPs have crystalline nature and also have some characteristic peaks.

Properties of snake venoms and TiO₂-NPs. LD₅₀ of DRV was found to be 2.2 µg intravenously and 45 µg when injected subcutaneously in mice (18–20 g); whereas NKV was 2.8 µg intravenously and 4.61 µg subcutaneously. The MHD/MND was 5 µg per animal (18–20 g) of DRV. MDD was 2.5 µg per animal (18–20 g) of DRV. The concentration of viper and cobra venoms in terms of protein were found to be 91.5% and 95% respectively. The TiO₂-NPs [up to 25 ng per animal (18–20 g); *i.v*] did not produce any lethal effect up to 48 hours of observations²².

Lethal activity. In *in-vitro* study, viper and cobra venoms (1–10 LD₅₀) were incubated with TiO₂-NPs (2 ng) and gave protection against venom-induced lethality. In *in vivo* study, cobra venom (1–5 LD₅₀) was injected (*s.c*) into male albino mice followed by TiO₂-NPs (5 ng/mouse, *i.v*). Viper and Cobra venom-induced lethality was significantly antagonized by TiO₂-NPs as compared with the control animal (venom only) (Table 1). The ED₅₀ of the TiO₂-NPs was observed as 2 ng *in vitro* and 4 ng in *in vivo* respectively against viper venom (Table 1).

Haemorrhagic and necrotic activity. In *in-vitro* study, Viper venom (20 µg) incubated with TiO₂ (2 ng) and injected 0.1 ml (*i.d*) into mice. It showed protection against venom induced haemorrhagic activity (Table 2). In *in-vivo* study, venom (10 µg) injected (*i.d*) into mice followed by the injection (*i.v*) of TiO₂-NPs (5 ng) gave protection against venom-induced haemorrhagic activity. The degree of protection in *in-vivo* was less than that of *in-vitro* studies.

Defibrinogenation activity. The TiO₂-NPs effectively antagonized the viper venom-induced defibrinogenating activity. In *in-vitro* study, the TiO₂-NPs (2 ng) gave protection up to 2 MDD (5 µg) against venom-induced defibrinogenation. In *in-vivo* study, venom-induced defibrinogenation was antagonised by TiO₂-NPs. The fold of protection was always higher in *in vitro* studies (Table 3).

Neutralisation of Venom Phospholipase A₂ (PLA₂) activity. Egg yolk coagulation method was performed to assess the PLA₂ activity of viper venom. 1 unit of venom activity which increased the coagulation time by 1 minute was found to be 2 µg (control 0.9% saline, coagulation time was found to be 45 ± 1.16 seconds). The TiO₂-NPs were tested for Phospholipase A₂ activity by incubating with different amount of venom (10 µg). The venom PLA₂ was effectively neutralized by the TiO₂-NPs (Table 4).

Mouse paw oedema. The assessment of anti-inflammatory activity of the TiO₂-NPs was done by mouse paw oedema. Mouse paw oedema was induced by venom, attained its peak at 1 hour of observation. The TiO₂-NPs at a dose of 5 ng/mouse (*i.p*) was found to produce significant inhibition of venom-induced inflammation. Inhibition of inflammation induced by TiO₂-NPs was maximum (51.3 ± 2.5%) at 2 hours of observation, as compared with

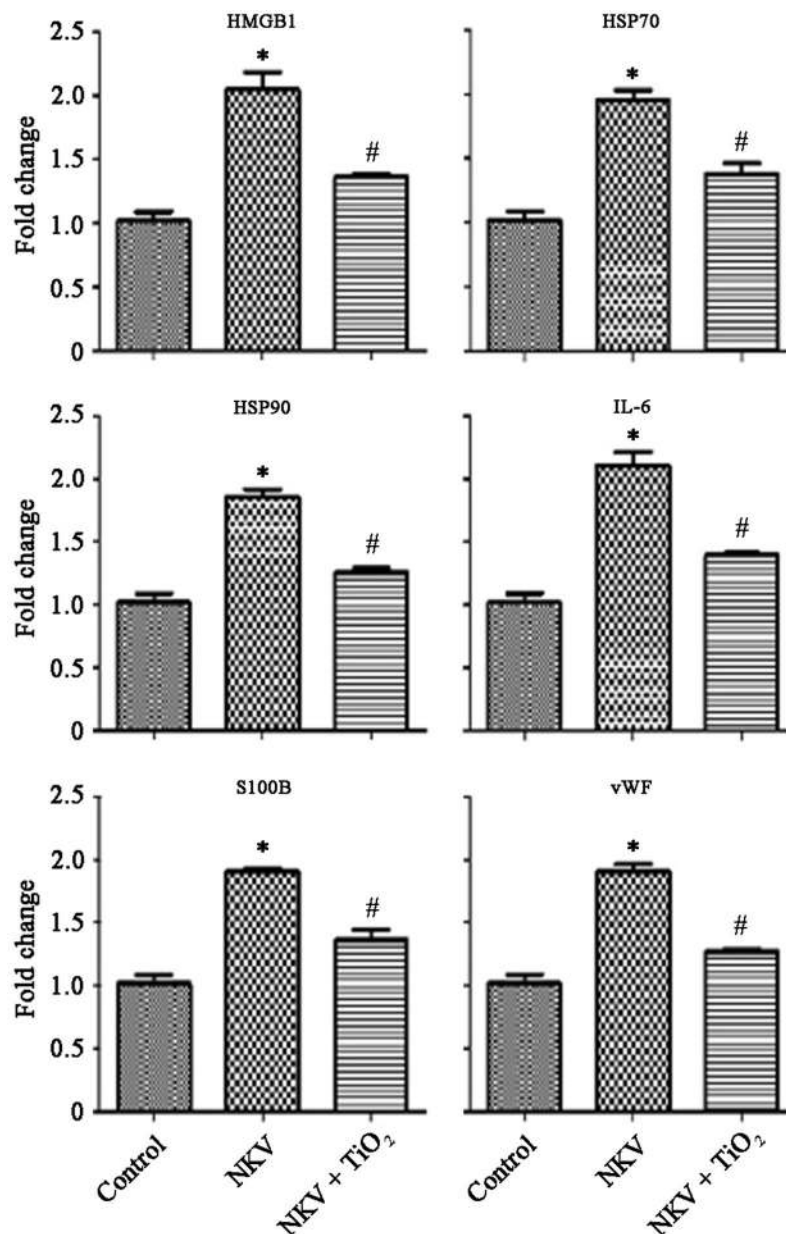


Figure 3. Cobra (*Naja kaouthia*) venom (NKV) induced inflammatory changes in experimental animals. Results expressed as mean \pm SEM (n = 6). Results obtained are significantly different from control group (* $P < 0.05$) and *Naja kaouthia* venom (# $P < 0.05$).

aspirin ($42.8 \pm 1.2\%$) and indomethacin ($40.3 \pm 1.3\%$). Carrageenan ($300 \mu\text{g}$ in 0.01 ml) injection produced significant inflammation in mouse paws. Pre-treatment with TiO_2 -NPs (5 mg/kg , *i.p.*) before carrageenan injection produced a significant reduction in oedema (Table 5).

Sterile inflammatory markers. The sterile inflammatory markers HMGB1, HSP70, HSP90, IL-6, S-100B and vWF were found to increase in Viper and Cobra venoms treated mouse while treatment with TiO_2 -NPs significantly reduced confirming the anti-inflammatory effects of TiO_2 -NPs (Figs 2 and 3).

Discussion

Injury and death due to snake bite is major health hazards in tropical and subtropical countries. In India more than 250 species of snakes are found, out of which 50 are venomous. Cobra and viper are the common snakes found throughout India^{32–34}. The majority of death occurs due to the bites of these snakes. Snake envenomation is characterized by severe damage caused by the toxic action of venom components. The venom contains multiple components that induce haemorrhage, necrosis, inflammation, nephrotoxicity, cardiotoxicity, hematoxicity and often leads to death^{35,36}. Viper and cobra venom contains major parts of Phospholipase A₂ (PLA₂) and metalloproteinase. Viper venom is a rich source of PLA₂ enzyme that leads to many pathophysiological disturbances in

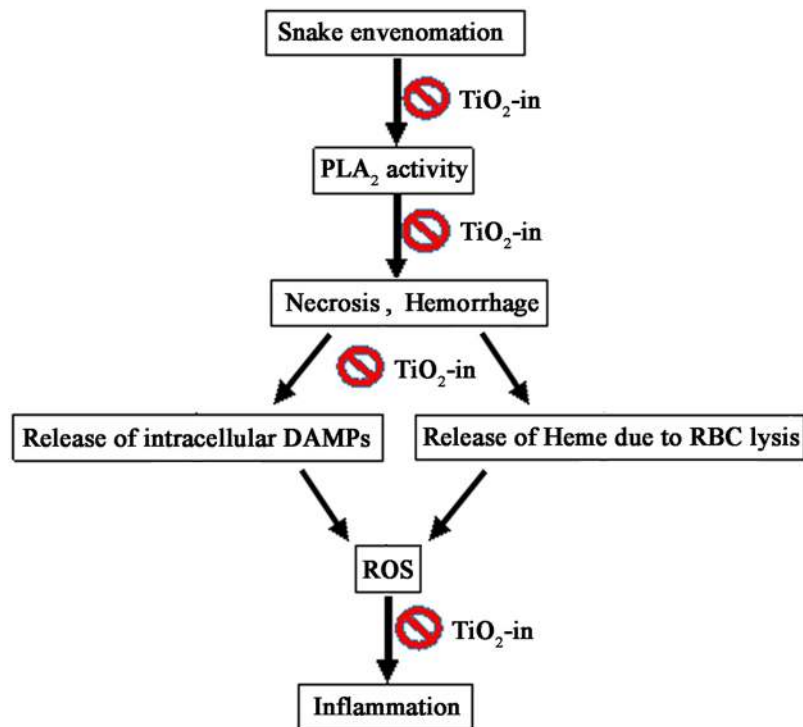


Figure 4. Possible mechanism of action of TiO₂ [TiO₂-in (inhibition)]. Snake venom-induced necrosis, haemorrhagic, lethal and inflammation and its neutralization by TiO₂-NPs.

the victims³⁴. These components directly damage the micro-vessels, with consequent increase in haemorrhage and oedema³⁴. The inflammatory effect induced by viper envenomation is due to the presence of PLA₂ enzyme in venom^{34–37}. The inflammatory effects induced by PLA₂ in response to cobra and viper venoms are primarily related to the action of this enzyme on the membrane phospholipids and the release of eicosanoid precursors^{25,38–42}. In present work, we characterized the oedematogenic, haemorrhagic, lethal and anti-inflammatory effects induced by the viper venom and its neutralization by TiO₂-NPs (Fig. 4). Nanomedicine is a rapidly evolving field that provide enhanced diagnostic imaging and treatment of diseases known as theranostic. On account of improved health care, theranostic approaches are employed to make drug delivery more efficient and target specific. Theranostic nanomedicine can also be used for different purposes like non-invasive assessment of the pharmacokinetics, bio-distribution and the target site localization of conjugated or entrapped active agents^{43,44}. Therefore TiO₂-NPs is considered as a suitable target for medicine delivery as well as for detection of target cells due to its high fluorescence property under the excitation of normal white light in *in vitro* condition.

In this study, we have shown that TiO₂-NPs are effective agent that may be used as a treatment in snake venom induced pathophysiological changes. TiO₂-NP arrays have been fabricated on p-type Si substrate using a cost effective (GLAD, PVD) technique. The surface topography revealed that the average size of TiO₂-NPs is in nano-metric range. The element mapping of FESEM image indicates the presence of Titanium (Ti) and Oxygen (O) in the sample. The stability of TiO₂-NPs synthesised by glancing angle deposition technique was calculated by its zeta potential. The continuous SAED analysis of TiO₂-NPs reveals that particles are having crystalline behaviour with fine stability. So far, we have seen that TiO₂-NPs effectively neutralize the viper and cobra venom-induced lethal activities both in *in vitro* and *in vivo* studies. TiO₂-NPs also effectively neutralized the viper venom induced haemorrhagic activity in experimental animals. The fold of venom induced lethal and haemorrhagic activity was always found to be higher in *in vitro* than *in vivo* studies. The TiO₂-NPs were also found to be more effective in viper venom induced pathophysiological changes than the cobra venom. The exact mechanism of action is still unclear. Among the several, one of the consequences of snake envenomation is increased DAMP molecules. Here, we have shown for the first time that the sterile inflammatory markers like IL-6, HSP, vWF, S100B and HMGB1 were increased by the administration of both cobra and viper venoms in male albino mice. The venoms may act through the stimulation of arachidonic acid pathway that leads to the generation of ROS and cytokines which leads to haemorrhage and tissue injury^{41,45,46}. Tissue injury caused due to snake envenomation could be because of different mechanism. One of the mechanisms is inflammatory response which entails the generation of Hsp70, Hsp90, HMGB1, IL6, vWF and S100b. They are all generated through the arachidonic acid pathway. The metabolism of arachidonic acid by lipo-oxygenase or cyclo-oxygenase causes the release of pro-inflammatory marker proteins. Presence of PLA₂ in viper venom helps in the conversion of the phospholipids to arachidonic acid which causes release of cytokines and leukotrienes^{25,47,48}. The TiO₂-NPs inhibits the production of sterile inflammatory proteins in venom-induced experimental rodents. The fold of protection is higher in case of viper venom than the cobra venom may be because of the difference in PLA₂ concentration. PLA₂ is

higher in viper venom than the cobra venom. Further study may provide new biological probes in the treatments of snakebite. TiO₂-NPs have shown better results in *in vitro* than in *in vivo* experiments. Our present investigation showed that the TiO₂-NPs is effective against venom-induced pathophysiological conditions and could be taken as a potential antidote. The present work may be helpful to treat victims of snakebite especially in rural parts of India where availability of antiserum is limited. We are engage to explore the mechanism of venom inhibition by TiO₂-NPs as a potential therapeutic agent against snake envenomation^{49,50}.

References

- Wang, L. S., Chuang, M. C. & Ho, J. A. Nanotheranostics—a review of recent publications. *Int J Nanomedicine* **7**, 4679–95 (2012).
- Sarkar, S., Alam, M. A., Shaw, J. & Dasgupta, A. K. Drug delivery using platelet cancer cell interaction. *Pharm Res* **30**, 2785–94 (2013).
- Drbohlavova, J., Adam, V., Kizek, R. & Hubalek, J. Quantum dots - characterization, preparation and usage in biological systems. *Int J Mol Sci.* **10**, 656–73 (2009).
- Mital, G. S. & Manoj, T. A review of TiO₂ nanoparticles. *Chinese Sci Bull.* **56**, 1639–57 (2011).
- Zhang, A. P. & Sun, Y. P. Photocatalytic killing effect of TiO₂ nanoparticles on Ls-174-t human colon carcinoma cells. *World J Gastroenterol.* **10**, 3191–93 (2004).
- Cai, R. *et al.* Induction of cytotoxicity by photoexcited TiO₂ particles. *Cancer Res.* **52**, 2346–48 (1992).
- Donachie, M. J. Titanium: A Technical Guide. 62–68 (ASM International, Metals Park, Ohio, 1988).
- Chen, X. & Mao, S. S. Titanium dioxide nanomaterials: synthesis, properties, modifications, and applications. *Chem Rev.* **107**, 2891–59 (2007).
- WHO. Neglected tropical diseases. Geneva: World Health Organization, 2017, http://www.who.int/neglected_diseases/diseases/en/ (accessed August 28, 2018).
- Chippaux, J. P. Snake-bites: appraisal of the global situation. *Bull World Health Organ.* **76**, 515–24 (1998).
- Gutiérrez, J. M. *et al.* Snakebite envenoming. *Nat Rev Dis Primers* **3**, 17079, <https://doi.org/10.1038/nrdp.2017.63> (2017).
- Longbottom, J. *et al.* Vulnerability to snakebite envenoming: a global mapping of hotspots. *Lancet* **392**, 673–84 (2018).
- Gutiérrez, J. M. *et al.* Neutralization of local tissue damage induced by *Bothrops asper* (terciopelo) snake venom. *Toxicon* **36**, 1529–38 (1998).
- Isbister, G. K. Procoagulant snake toxins: laboratory studies, diagnosis, and understanding snakebite coagulopathy. *Semin Thromb Hemost.* **35**, 93–103 (2009).
- Queiroz, G. P. *et al.* Interspecific variation in venom composition and toxicity of Brazilian snakes from *Bothrops* genus. *Toxicon* **52**, 842–51 (2008).
- Stahel, E., Wellauer, R. & Freyvogel, T. A. Poisoning by domestic vipers (*Viperaberus* and *Viperaaspis*). A retrospective study of 113 patients [Article in German]. *Schweiz Med Wochenschr.* **115**, 890–96 (1985).
- Sutherland, S. K. Serum reactions. An analysis of commercial antivenoms and the possible role of anticomplementary activity in de-novo reactions to antivenoms and antitoxins. *Med J Aust.* **1**, 613–15 (1977).
- Cai, W. & Chen, X. Nano platforms for targeted molecular imaging in living subjects. *Small* **3**, 1840–54 (2007).
- Goswami, T., Mondal, A., Singh, P. & Choudhuri, B. In2-XO3-Y 1D perpendicular nanostructure arrays as ultraviolet detector. *Solid State Sciences* **48**, 56–60 (2015).
- Mondal, A., Ganguly, A., Das, A., Choudhuri, B. & Yadav, R. K. The Ag nanoparticles/TiO₂ thin film device for enhanced photoconduction and role of traps. *Plasmonics* **10**, 667–73 (2015).
- Alam, M. I. & Gomes, A. An experimental study on evaluation of chemical antagonists induced snake venom neutralization. *Indian J Med Res.* **107**, 142–46 (1998).
- Alam, M. I. & Gomes, A. Indian medicinal plants active against Elapidae and Viperidae snake venoms. *Toxicon* **34**, 155–56 (1996).
- Theakston, R. D. & Reid, H. A. Development of simple standard assay procedures for the characterization of snake venom. *Bull World Health Organ.* **61**, 949–56 (1983).
- Alam, M. I. & Gomes, A. Snake venom neutralization by Indian medicinal plants (*Vitex negundo* and *Embllica officinalis*) root extracts. *J Ethnopharmacol.* **86**, 75–80 (2003).
- Alam, M. I. & Gomes, A. Viper venom-induced inflammation and inhibition of free radical formation by pure compound (2-hydroxy-4-methoxy benzoic acid) isolated and purified from anantamul (*Hemidesmus indicus* R. BR) root extract. *Toxicon* **36**, 207–215 (1998).
- Alam, M. I. *et al.* Molecular modeling and snake venom phospholipase A₂ inhibition by phenolic compounds: Structure-activity relationship. *Eur J Med Chem.* **114**, 209–19 (2016).
- Habermann, E. & Neuman, W. Egg yolk coagulation method. *Physiol. Chem.* **297**, 174–176 (1954).
- Trebien, H. A. & Calixto, J. B. Pharmacological evaluation of rat paw oedema induced by *Bothrops jararaca* venom. *Agents Actions.* **26**, 292–300 (1989).
- Engvall, E. & Perlmann, P. Enzyme-linked immunosorbent assay, Elisa. 3. Quantitation of specific antibodies by enzyme-labeled anti-immunoglobulin in antigen-coated tubes. *J Immunol.* **109**, 129–35 (1972).
- Ilie, A. G. *et al.* Principal component analysis of Raman spectra for TiO₂ nanoparticle characterization. *Appl. Surf. Sci.* **417**, 93–103 (2017).
- Li, Y. S. & Church, J. S. Raman spectroscopy in the analysis of food and pharmaceutical nanomaterials. *J Food Drug Anal.* **22**, 29–48 (2014).
- Monteiro, F. N. *et al.* Clinico-epidemiological features of viper bite envenomation: a study from Manipal, South India. *Singapore Med J.* **53**, 203–07 (2012).
- Whitaker, R. Common Indian snakes: a field guide (ed. Whitaker, R.) 52–72 (Macmillan India, 2002).
- Chippaux, J. P. Snakebite envenomation turns again into a neglected tropical disease! *J Venom Anim Toxins Incl Trop Dis.* **23**, <https://doi.org/10.1186/s40409-017-0127-6> (2017).
- Gutiérrez, J. M., Theakston, R. D. & Warrell, D. A. Confronting the neglected problem of snake bite envenoming: the need for a global partnership. *PLoS Med.* **3**, e150, <https://doi.org/10.1371/journal.pmed.0030150> (2006).
- Sunitha, K. *et al.* Inflammation and oxidative stress in viper bite: an insight within and beyond. *Toxicon* **98**, 89–97 (2015).
- Markland, F. S. & Swenson, S. Snake venom metalloproteinases. *Toxicon* **62**, 3–18 (2013).
- Galvão Nascimento, N., Sampaio, M. C., Amaral Olivo, R. & Teixeira, C. Contribution of mast cells to the oedema induced by *Bothrops moojeni* snake venom and a pharmacological assessment of the inflammatory mediators involved. *Toxicon* **55**, 343–52 (2010).
- Fernandes, C. A., Borges, R. J., Lomonte, B. & Fontes, M. R. A structure-based proposal for a comprehensive myotoxic mechanism of phospholipase A₂-like proteins from viperid snake venoms. *Biochim Biophys Acta* **1844**, 2265–76 (2014).
- Dennis, E. A. Diversity of group types, regulation, and function of phospholipase A₂. *J Biol Chem.* **269**, 13057–60 (1994).
- Teixeira, C. F., Landucci, E. C., Antunes, E., Chacur, M. & Cury, Y. Inflammatory effects of snake venom myotoxic phospholipases A₂. *Toxicon.* **42**, 947–62 (2003).

42. Gutiérrez, J. M. & Ownby, C. L. Skeletal muscle degeneration induced by venom phospholipases A₂: insights into the mechanisms of local and systemic myotoxicity. *Toxicon* **42**, 915–31 (2003).
43. Cardoso, K. C. *et al.* A transcriptomic analysis of gene expression in the venom gland of the snake *Bothrops alternatus* (urutu). *BMC Genomics* **11**, 605, <https://doi.org/10.1186/1471-2164-11-605> (2010).
44. Lima, J. S. *et al.* Profile of snakebite accidents in the north of the State of Minas Gerais, Brazil. *Rev Soc Bras Med Trop.* **42**, 561–64 (2009).
45. Moulton, K. S. Angiogenesis in atherosclerosis: gathering evidence beyond speculation. *Curr Opin Lipidol.* **17**, 548–55 (2006).
46. Lanza, G. M. *et al.* Theragnostics for tumor and plaque angiogenesis with perfluorocarbon nanoemulsions. *Angiogenesis* **13**, 189–202 (2010).
47. Rainsford, K. Side-effects of anti-inflammatory/analgesic drugs: epidemiology and gastrointestinal tract. *Trends Pharmacol. Sci.* **5**, 156–59 (1984).
48. Barone, J. M., Alpointi, R. F., Frezzatti, R., Zambotti-Villela, L. & Silveira, P. F. Differential efficiency of simvastatin and lipoic acid treatments on *Bothrops jararaca* envenomation-induced acute kidney injury in mice. *Toxicon* **57**, 148–56 (2011).
49. Harris, J. B. Myotoxic phospholipases A₂ and the regeneration of skeletal muscles. *Toxicon* **42**, 933–45 (2003).
50. Voronov, E., Apte, R. N. & Sofer, S. The systemic inflammatory response syndrome related to the release of cytokines following severe envenomation. *J. Venom. Anim. Toxins* **5**, 5–33 (1999).

Acknowledgements

We would like to thank Dr. GN Qazi, Director General, HIMSR, Jamia Hamdard, New Delhi for his valuable inputs and support.

Author Contributions

The research was conceived and planned by M.I.A. S.C. performed the synthesis and characterization experiments. M.I.A. and G.A.K. helped in designing the animal experiments. M.I.A. and S.B. performed the *in vitro* animal experiments. M.I.A. and N.D. wrote the manuscript. A.A. helps in constructing the manuscript including figures and tables. M.S.A. provided the intellectual support. All authors read and approved the final manuscript and have no conflict of interests.

Additional Information

Competing Interests: The authors declare no competing interests.

Publisher's note: Springer Nature remains neutral with regard to jurisdictional claims in published maps and institutional affiliations.



Open Access This article is licensed under a Creative Commons Attribution 4.0 International License, which permits use, sharing, adaptation, distribution and reproduction in any medium or format, as long as you give appropriate credit to the original author(s) and the source, provide a link to the Creative Commons license, and indicate if changes were made. The images or other third party material in this article are included in the article's Creative Commons license, unless indicated otherwise in a credit line to the material. If material is not included in the article's Creative Commons license and your intended use is not permitted by statutory regulation or exceeds the permitted use, you will need to obtain permission directly from the copyright holder. To view a copy of this license, visit <http://creativecommons.org/licenses/by/4.0/>.

© The Author(s) 2019